Regular and chaotic classical dynamics in the U(5)-SU(3) quantum phase transition of the IBM

M. Macek and A. Leviatan

Citation: AIP Conf. Proc. **1488**, 441 (2012); doi: 10.1063/1.4759429
View online: http://dx.doi.org/10.1063/1.4759429
View Table of Contents: http://proceedings.aip.org/dbt/dbt.jsp?KEY=APCPCS&Volume=1488&Issue=1
Published by the American Institute of Physics.

Regular and chaotic classical dynamics in the U(5)-SU(3) quantum phase transition of the IBM

M. Macek and A. Leviatan

Racah Institute of Physics, The Hebrew University, Jerusalem 91904, Israel

Abstract. We study the classical dynamics in a generic first-order quantum phase transition between the U(5) and SU(3) limits of the interacting boson model. The dynamics is chaotic, of Hénon-Heiles type, in the spherical phase and is regular, yet sensitive to local degeneracies, in the deformed phase. Both types of dynamics persist in the coexistence region resulting in a divided phase space.

Keywords: First order quantum phase transition, classical chaos, mixed dynamics
PACS: 21.60.Fw, 05.30.Rt, 05.45.Ac, 05.45.Pq

The interacting boson model (IBM) [1] describes quadrupole collective states in even-even nuclei in terms of a system of N monopole (s) and quadrupole (d) bosons, representing valence nucleon pairs. In addition to its traditional role of interpreting spectroscopic data, the model provides a fertile ground for studying quantum phase transitions (QPTs) and mixed regular/chaotic dynamics in a mesoscopic (finite) system. QPTs refer to structural changes induced by a change of parameters λ in the quantum Hamiltonian, $\hat{H}(\lambda)$. The underlying mean-field (Landau) potential, $V(\lambda)$, determines the nature of the QPT. In particular, for discontinuous (first-order) QPTs, $V(\lambda)$ develops multiple minima that coexist in a range of λ values and cross at the critical point, $\lambda = \lambda_c$. In the IBM, the integrable dynamical symmetry (DS) limits relate to stable structural phases and QPTs are obtained by mixing terms from different DS chains [2]. The competing interactions that drive these QPTs can affect dramatically the nature of the dynamics and, in some cases, lead to the emergence of quantum chaos.

QPTs [2, 3, 4] and chaos [5, 6] have been studied extensively in the IBM, albeit, with a simplified Hamiltonian which, for first-order QPTs, gave rise to extremely low barrier and narrow coexistence region. Recently, the identification of IBM Hamiltonians without such restrictions [7], enabled a comprehensive analysis of generic first-order QPTs between spherical and deformed shapes [8, 9, 10]. The dynamics inside the phase coexistence region was found to exhibit a very simple pattern. A classical analysis revealed a robustly regular dynamics confined to the deformed region and well separated from a chaotic dynamics ascribed to the spherical region. This divided phase space structure manifests itself also in the quantum analysis, disclosing regular rotational bands in the deformed region amidst a complicated environment. In the present contribution, we illuminate the origin of this intricate interplay of order and chaos for a particular case, where the stable spherical and deformed phases posses U(5) and SU(3) DS, respectively.

Apart from kinetic rotational terms, the relevant Hamiltonian (up to a scale) is

$$\hat{H}_1(\rho) = 2(1-2\rho^2)\hat{n}_d(\hat{n}_d-1) + 2R_2^\dagger(\rho)\cdot\tilde{R}_2(\rho)\,, \quad (1)$$

$$\hat{H}_2(\xi) = \xi P_0^\dagger P_0 + P_2^\dagger\cdot\tilde{P}_2\,. \quad (2)$$

Beauty in Physics: Theory and Experiment
AIP Conf. Proc. 1488, 441-444 (2012); doi: 10.1063/1.4759429

Here $\hat{n}_d$ is the d-boson number operator, $R^{\dagger}_{2\mu}(\rho) = \sqrt{2}s^{\dagger}d^{\dagger}_{\mu} + \rho\sqrt{7}(d^{\dagger}d^{\dagger})^{(2)}_{\mu}$, $P^{\dagger}_0 = d^{\dagger}\cdot d^{\dagger} - 2(s^{\dagger})^2$, $P^{\dagger}_{2\mu} = 2s^{\dagger}d^{\dagger}_{\mu} + \sqrt{7}(d^{\dagger}d^{\dagger})^{(2)}_{\mu}$ and the centered dot implies a scalar product. The parameters that control the QPT are ρ and ξ, with $0 \leq \rho \leq 1/\sqrt{2}$ and $\xi \geq 0$. For $\rho = 0$ and $\xi = 1$, one recovers the U(5) and SU(3) DS limits, where the Hamiltonians

$$\hat{H}_1(\rho = 0) = 2\hat{n}_d[2\hat{N} - \hat{n}_d - 1] \,, \tag{3}$$

$$\hat{H}_2(\xi = 1) = [-\hat{C}_{\mathrm{SU(3)}} + 2\hat{N}(2\hat{N} + 3)] \,, \tag{4}$$

involve the relevant Casimir operators. The two Hamiltonians of Eqs. (1)-(2) coincide at the critical point $\rho_c = 1/\sqrt{2}$ and $\xi_c = 0$: $\hat{H}_1(\rho_c) = \hat{H}_2(\xi_c)$.

The classical limit is obtained through the use of coherent states, rescaling and taking $N \to \infty$, with $1/N$ playing the role of $\hbar$. The derived classical Hamiltonians, $\mathscr{H}_1(\rho)$, $\mathscr{H}_2(\xi)$, involve complicated expressions of shape variables (β, γ), Euler angles and their conjugate momenta. Setting the latter to zero, yields the following classical potentials

$$V_1(\rho) = 2\beta^2 - \beta^4/2 - 2\rho\sqrt{2 - \beta^2}\beta^3 \cos 3\gamma \,, \tag{5}$$

$$V_2(\xi) = \xi\left(4 - 6\beta^2 + 9\beta^4/4\right) + 2\beta^2 - \beta^4/2 - \sqrt{4 - 2\beta^2}\beta^3 \cos 3\gamma \,. \tag{6}$$

$V_1(\rho)$ and $V_2(\xi)$ serve as the Landau potentials with the equilibrium deformations $(\beta_{\mathrm{eq}}, \gamma_{\mathrm{eq}})$ as order parameters. The potential $V_1(\rho)$ [$V_2(\xi)$] has a global spherical [deformed] minimum with, respectively, $\beta_{\mathrm{eq}} = 0$ [$\beta_{\mathrm{eq}} = 2/\sqrt{3}, \gamma_{\mathrm{eq}} = 0$]. At the spinodal point ($\rho^* = 1/2$), $V_1(\rho)$ develops an additional local deformed minimum. The two minima become degenerate at the critical point $\rho_c = 1/\sqrt{2}$ (or $\xi_c = 0$), and are separated by a barrier of height $V_b = 0.268$ (compared to $V_b = 0.0018$ in previous works [5]). The spherical minimum turns local in $V_2(\xi)$ for $\xi > \xi_c$ and disappears at the anti-spinodal point ($\xi^{**} = 1/3$). The order parameter β_{eq}, is a double-valued function in the coexistence region (in-between ρ^* and ξ^{**}) and a step-function outside it.

The classical analysis simplifies considerably when the dynamics is restricted to $L = 0$ vibrations. In this case, the classical Hamiltonians, $\mathscr{H}_1(\rho)$, $\mathscr{H}_2(\xi)$, become two-dimensional in the polar coordinates $\beta \in [0, \sqrt{2}]$, $\gamma \in [0, 2\pi)$ and momenta $p_\beta \in [0, \sqrt{2}]$, $p_\gamma \in [0, 1]$ (or, equivalently, in Cartesian coordinates, $x = \beta\cos\gamma$, $y = \beta\sin\gamma$ and p_x, p_y). The classical motion can then be depicted conveniently via Poincaré surfaces of section [11], shown at prescribed energies in Figs. 1-2, along with selected trajectories.

The classical dynamics on the spherical side of the QPT ($0 \leq \rho \leq \rho_c$), is governed by $\mathscr{H}_1(\rho)$. In the U(5) limit ($\rho = 0$), the system is integrable and $\mathscr{H}_1(\rho = 0) = 2(T + \beta^2) - (T + \beta^2)^2/2$, where $T = p^2_\beta + \beta^{-2}p^2_\gamma$. As shown in Fig. 1(a), the sections, for small ρ, show the phase space portrait typical of a weakly perturbed anharmonic (quartic) oscillator with two major regular islands and quasi-periodic trajectories. The effect of increasing ρ on the dynamics in the vicinity of the spherical minimum ($x \approx 0$), can be inferred from a small β-expansion of the potential, $V_1(\rho) \approx 2\beta^2 - 2\rho\sqrt{2}\beta^3\cos 3\gamma$. To this order, $V_1(\rho)$ coincides with the well-known Hénon-Heiles (HH) potential [12]. As shown for $\rho = 0.2$, at low energy [Fig. 1(b)], the dynamics remains regular, and two additional islands show up. At higher energy [Fig. 1(c)], one observes a marked

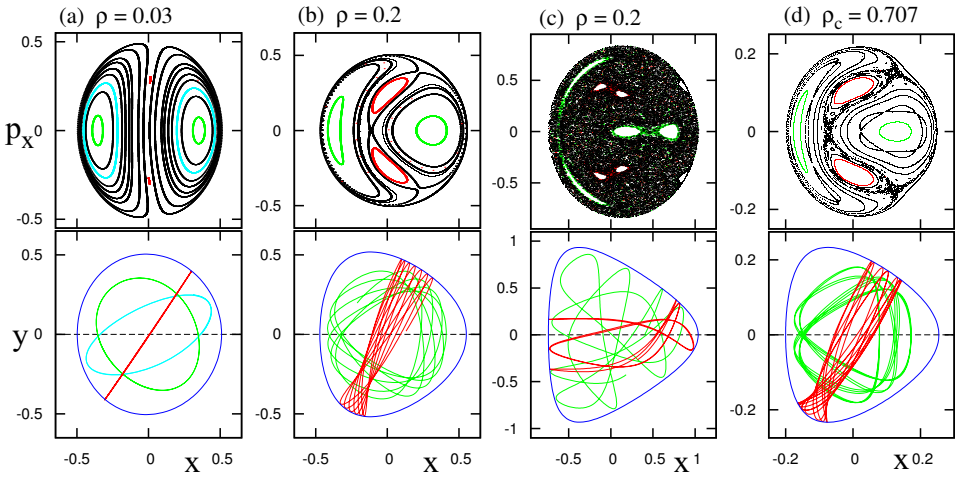

FIGURE 1. Poincaré sections (top row), plotted at $y = 0$, and selected trajectories (bottom row), depicting the classical dynamics of $\hat{H}_1(\rho)$ (1) for several values of ρ and energies E. (a) $\rho = 0.03$, $E = E_1/21$. (b) $\rho = 0.2$, $E = 5E_1/12$. (c) $\rho = 0.2$, $E = 12E_1/21$. (d) $\rho_c = 1/\sqrt{2}$, $E = E_1/12$ (the critical point). The energies are given with respect to the domain boundary $E_1 \equiv V_1(\rho;\beta = \sqrt{2}) = 2$.

onset of chaos and an ergodic domain. The energy where the order-to-chaos transition occurs decreases with ρ. This typical HH-type of behaviour persists in the vicinity of the spherical minimum throughout the coexistence region, including the critical point [Fig. 1(d)]. It is also present in the region where the spherical minimum is only local ($0 \leq \xi \leq \xi^{**}$), since $V_2(\xi) \approx 4\xi + (2-6\xi)\beta^2 - 2\beta^3 \cos 3\gamma$.

The classical dynamics on the deformed side of the QPT ($\xi_c \leq \xi \leq 1$), is governed by $\mathscr{H}_2(\xi)$ and has a very different character, being robustly regular in the vicinity of the deformed minimum ($x \approx 1$). At low energy, the motion reflects the β and γ normal mode oscillations about the minimum. As shown in Fig. 2(a), the trajectories form a single set of concentric loops around a single stable (elliptic) fixed point. They portray γ-vibrations at the center of the surface ($p_x \approx 0$) and β-vibrations at the perimeter (large $|p_x|$). This regular pattern of the dynamics is found for most values of $\xi \geq 0$ both inside and outside the phase coexistence region. Noticeable exceptions occur in the presence of resonances, which appear when the ratio of normal mode frequencies, $R \equiv \varepsilon_\beta/\varepsilon_\gamma$, is a rational number. At low energy, this happens at discrete values of the control parameter $\xi \approx \xi_R$, in a narrow interval around $\xi_R = (3R-1)/2$. Panels (b)-(c)-(d) of Fig. 2 show examples of such scenario for $R = 1/2, 2/3, 1$. The corresponding surfaces exhibit four, three and two KAM islands, respectively. The phase space portrait for ($\xi = 1, R = 1$), shown in Fig. 2(d), corresponds to the integrable SU(3) DS limit, Eq. (4), and is the same for any energy. Interestingly, in the coexistence region, where the Landau potential accommodates both the spherical and deformed minima, each minimum preserves its own characteristic dynamics. This is evident in Fig. 1(d) and Fig. 2(a), which depict the dynamics of the same system [$\hat{H}_1(\rho_c) = \hat{H}_2(\xi_c)$] at the same energy, but in different regions (x-ranges) of phase space.

In summary, we have shown the distinct morphology of classical orbits and different onset of regularity and chaos in a generic (high-barrier) first-order QPT between the

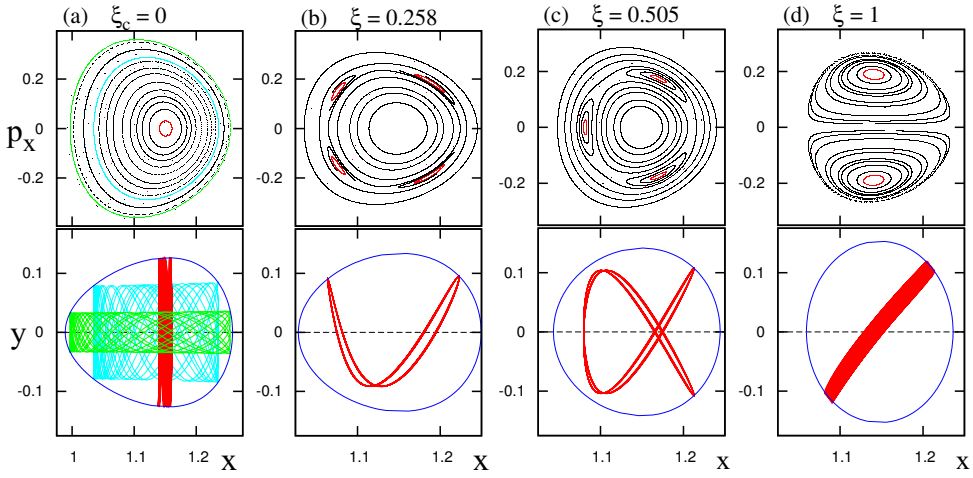

FIGURE 2. Same as in Fig. 1 but for the classical dynamics of $\hat{H}_2(\xi)$ (2) for selected values of ξ and energy $E = E_2/21$, where $E_2 = V_2(\xi;\beta=\sqrt{2}) = 2+\xi$. Panel (a) shows a typical pattern encountered for most values of $\xi \geq 0$. Panels (b)-(c)-(d) portray the surfaces in the presence of local degeneracies of normal modes, $\varepsilon_\beta/\varepsilon_\gamma = 1/2, 2/3, 1$, respectively. Panel (d) corresponds to the SU(3) DS limit, Eq. (4).

U(5) [spherical] and SU(3) [deformed] phases of the IBM. The spherical phase displays a chaos-susceptible dynamics, similar to the Hénon-Heiles system, due to a $\beta^3 \cos 3\gamma$ perturbation, significant near the spherical minimum. In contrast, the low energy dynamics in the deformed phase is robustly ordered, and reflects the β-γ vibrations about the deformed minimum. This regular dynamics is sensitive to local degeneracies of these normal modes. The two types of dynamics preserve their identity and can be detected as long as the relevant minimum exists. This leads to a divided phase space structure throughout the phase-coexistence region, as found in [8, 9, 10].

This work is supported by the Israel Science Foundation. M.M. acknowledges support by the Golda Meir Fellowship Fund and the Czech Ministry of Education (MSM 0021620859).

REFERENCES

1. F. Iachello, and A. Arima, *The Interacting Boson Model*, Cambridge Univ. Press, Cambridge, 1987.
2. A.E.L. Dieperink, O. Scholten, and F. Iachello, *Phys. Rev. Lett.* **44**, 1747 (1980).
3. P. Cejnar, and J. Jolie, *Prog. Part. Nucl. Phys.* **62**, 210 (2009).
4. F. Iachello, *Rivista Del Nuovo Cimento* **34**, 617 (2011).
5. N. Whelan, and Y. Alhassid, *Nucl. Phys. A* **556**, 42 (1993).
6. M. Macek, P. Stránský, P. Cejnar, S. Heinze, J. Jolie, and J. Dobeš, *Phys. Rev. C* **75**, 064318 (2007).
7. A. Leviatan, *Phys. Rev. C* **74**, 051301 (2006).
8. M. Macek, and A. Leviatan, *Phys. Rev. C* **84**, 041302(R) (2011).
9. A. Leviatan, and M. Macek, *Phys. Lett. B* **714**, 110 (2012).
10. M. Macek, and A. Leviatan (2012), in preparation.
11. M. C. Gutzwiller, *Chaos in Classical and Quantum Mechanics*, Springer, New York, 1990.
12. M. Hénon, and C. Heiles, *Astron. J.* **69**, 73 (1964).